Nuclear Instruments and Methods in Physics Research B 354 (2015) 37–41

Contents lists available at ScienceDirect

Nuclear Instruments and Methods in Physics Research B

journal homepage: www.elsevier.com/locate/nimb

Electron scattering as a tool to study zero-point kinetic energies of atoms in molecules

R. Moreh [a,*], Y. Finkelstein [b], M. Vos [c]

[a] Physics Department, Ben-Gurion University of the Negev, Beer-Sheva 84105, Israel
[b] Nuclear Research Center – Negev, Beer-Sheva 84190, Israel
[c] Atomic and Molecular Physics Laboratories, Australian National University, Canberra, Australia

ARTICLE INFO

Article history:
Received 5 August 2014
Received in revised form 21 November 2014
Accepted 24 November 2014
Available online 6 December 2014

Keywords:
Electron compton scattering
Atomic kinetic energy
H_2
NH_3
H_2O

ABSTRACT

High resolution electron compton scattering (ECS) is being used to study the atomic momentum distributions and hence the zero-point kinetic energies (ZPKE) of the scattering atoms. Such studies have shown that the scattering is from a single atom of the scattering sample. For an electron beam with a well defined incident energy, the scattered electron energy at any angle from each atomic species is Doppler broadened. The broadening reflects the atomic momentum distribution contributed by both the internal and external motions of the molecular system. By measuring the Doppler broadening of the scattered electron lines it was possible to determine the kinetic energy of the scattering atom including that of its zero-point motion. Thus, the atomic kinetic energies in gases such as H_2, D_2, HD, CH_4 and in H_2O, D_2O and NH_3 were measured and compared with those calculated semi-empirically using the measured optical infra red (IR) and Raman frequencies of the internal vibrations of the molecules. In general, good agreement between the measured and calculated values was found. Electron scattering was also used to study the ratio of e-scattering intensities from the H- and O-atoms in water (H_2O), where some anomalies were reported to exist.

© 2014 Elsevier B.V. All rights reserved.

1. Introduction

In recent years many scattering studies were carried out using electron beams with incident energies between 1 and 40 keV. The targets were in various forms and the electrons were found to scatter independently from each atomic mass and not from the molecule as a whole. This behavior is contained in the assumption of the impulse approximation (IA) found to hold in many cases studied using the electron scattering method; it is due to the high incident electron energies compared to the vibrational energy of the atoms in the samples.

Few methods were reported in the literature in which a direct measurement of the atomic kinetic energies was carried out: (1) Nuclear resonance photon scattering (NRPS) [1], (2) neutron compton scattering (NCS) [2,3], and (3) electron compton scattering (ECS) [4–6]. Here we use the abbreviation ECS, to emphasize the similarities with the well-established NCS technique. When the same technique is used for determination of the composition of surfaces, it is often referred to as electron Rutherford Backscattering (ERBS). The same spectrometer can study electronic excitations, in which case the technique is called reflection energy loss spectroscopy (RELS). The NRPS method used either gamma rays (emitted from thermal neutron capture reactions on various elements) or bremsstrahlung photons created by 4–10 MeV electrons striking a high-Z target. In the first case a nuclear reactor was employed to provide the high flux of neutrons for producing the intense photon beam; it was used extensively for several applications [1,7–9]. The other case employed an electron Linac to produce the high intensity bremsstrahlung beam [10].

The second method using NCS was found to have several properties in common with ECS in the sense that the neutron scatters from an atom in a molecule as if it was free, thus the kinematics in the two cases are quite similar. In fact, the atomic kinetic energies measured by the two methods were found in many cases to be close to each other. Moreover, as mentioned below, it was possible to check some anomalies reported by the NCS method [11–14]; the result was that those anomalies did not persist using the ECS technique [15].

The atomic kinetic energies in molecules and in solids were calculated using a semi-empirical (SE) method [1,16] in which the vibrational frequencies are taken from experiment and it is assumed that there is no coupling between the different modes

* Corresponding author.
E-mail address: moreh@bgu.ac.il (R. Moreh).

http://dx.doi.org/10.1016/j.nimb.2014.11.078
0168-583X/© 2014 Elsevier B.V. All rights reserved.

of motion. This method was found to yield in several cases the best and the closest agreement to experiment.

Because of the small electron mass, the recoil energy transferred to the scattering atom is very small [17–19]. Thus, the scattering process operates as a mass analyzer causing the energy spectrum of the deflected electrons to split according to the masses of the scattering atoms of the molecule. In order for the energy separations between the scattering peaks to be resolved, a high resolution spectrometer had to be used [4]. The Doppler broadening $\Delta = (4K_eE_{rec})^{1/2}$ of each electron line is related to the mean kinetic energy K_e of the scattering atom and to the recoil energy E_{rec}; it provides information on K_e in the same fashion as that of NCS [19].

The measurement of the K_e of a scattering atom in a molecule is important as it includes the part contributed by the zero-point vibrational motion and may be obtained by measuring the Doppler broadening of the scattered electron lines. In any H-containing molecule the internal kinetic energy is carried mostly by the light partner, i.e. the H-atom and can be measured with good accuracy as in NH_3, H_2O, CH_4 (see below).

2. Experimental details

In the measurements, an electron beam with a well defined incident energy between 1 to 40 keV and low thermal spread was used. The energy analysis of the scattered electrons requires spectrometers of very high resolution to resolve the small difference in recoil energy of the atoms present as well as the total energy spread of the electrons scattered from a specific isotope. The energy resolution of our spectrometer is 0.3 eV; it includes the thermal spread of the electrons emitted from a barium oxide cathode. Besides the experimental resolution the energy of the scattered electron is affected by the Doppler broadening caused by the internal and external motions of the atoms of the sample. This is the quantity we want to measure. Fig. 1 depicts the Doppler broadened shape of electrons scattered at 135° from the H-atom (of a solid ammonia (NH_3) sample) at 80 K using a 2.5 keV incident e-beam. It shows the energy separation between the peak intensities of the electrons scattered from N- and H-atoms in NH_3, illustrating the type of resolution required in such measurements [4]. As the N peak is much narrower than the H peak, it is immediately clear that the width of the latter is dominated by Doppler broadening. Apart from NH_3, the samples discussed in this work are H_2, HD, D_2, CH_4 and H_2O. The electron incident energies employed in the studies discussed here were between 1 and 6 keV.

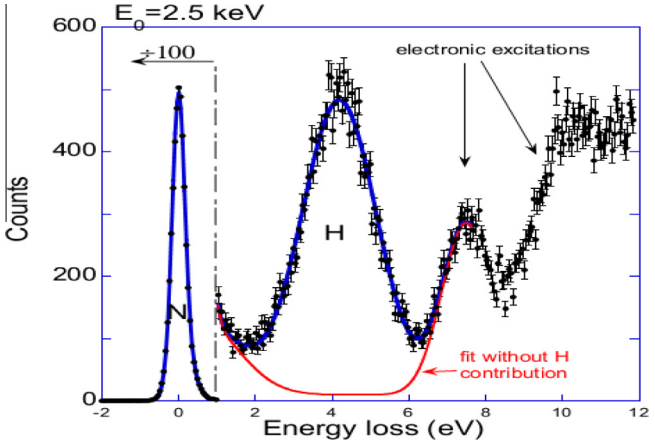

Fig. 1. Spectrum of 2.5 keV electrons scattered over 135° from a solid ammonia (NH_3) sample at 80 K. It illustrates the energy separation between the N- and H-atoms and the Doppler broadened shapes of the peaks. It also shows the fitting procedure and assumed background due to detected electrons that have also created electronic excitations in the target.

Gas phase measurements are near room temperature as the pressure differential over the nozzle is small and adiabatic cooling should thus be minor. The low temperature measurements are made from frozen samples using either a cold finger (H_2O case at 118 K) or a LN_2 cryostat (NH_3 case at ~80 K). From the spectra we determined the intrinsic width (Doppler broadening Δ) of the peaks (by subtracting the experimental resolution from the observed width in quadrature) and for isotropic systems the intrinsic width is related to the mean kinetic energy K_e according to [6]: $\Delta = \sqrt{\frac{4}{3}K_eE_{rec}}$. With E_{rec} the recoil energy for scattering from a stationary atom.

In the following we explain how the atomic kinetic energies were calculated.

3. Calculations and results

3.1. Diatomic gases

As an example we show how to calculate the H-kinetic energy, K_e(H), in a diatomic molecule such as HD in gaseous phase. Note that K_e(H) is contributed by three components: Translation, *free* rotation and internal vibration of the molecule. By assuming a decoupling of the three motions, and using the harmonic approximation, we may write [1,16]:

$$K_e(\mathrm{H}) = S_t\frac{3}{2}kT + S_rkT + S_v\frac{h\upsilon_0}{2}\left(\frac{1}{e^{h\nu_0/kT}-1}+\frac{1}{2}\right) \quad (1)$$

where S_t, S_r and S_v are the kinetic energy fractions shared by the H-atom in the translational, rotational and vibrational motions of the H-atom in the HD molecule respectively. Here, the vibrational motion of HD is represented by a harmonic quantum oscillator with frequency ν_0 (taken from experiment) [20]. Eq. (1) may be viewed as representing the kinetic energy of any isotope in H_2, HD and D_2. The energy fractions of Eq. (1) for those isotopic gases are listed in Table 1 from which the atomic kinetic energies of H and D were calculated (Table 1). It was assumed that the D mass is twice the H-mass and that the spring constant of the oscillator is the same for the three gases. As expected, the calculated K_e(H) in H_2 is smaller than that in HD but higher than K_e(D) in D_2 as well as in HD. This may be understood by noting that the oscillator kinetic energy in HD is divided between the H- and D-masses in a 2:1 ratio. Table 1 also lists the calculated K_e(H) values at 145 K and 0 K. Note that the zero-point value was calculated by accounting for the contributions from both the external-lattice and the internal motions, while in the gaseous phase where the molecule freely rotates, the major contribution to K_e is from the internal vibration. In HD at 145 K for example, the major part, 84% of K_e(H) = 89.1 meV, is contributed by the zero-point motion of the

Table 1
Calculated energy fractions S_t, S_r, S_v together with the kinetic energies, K_e(H) and K_e(D), at 0 K and 145 K of H_2, HD and D_2. Values of the experimental frequency ν_0 are also listed together with the *measured* K_e values using the ECS method. Indicated in the last column are the calculated total zero point energies (bold) of the H and D atoms, which include contributions from both external lattice and internal modes of motion, where the lattice modes were calculated assuming a pure Debye solid [22]. Parenthesized italics values are the calculated zero point energies of the internal vibrations obtained using Eq. (1).

Gas	S_t	S_r	S_v	ν_0 [cm^{-1}]	K_e(H,D) [meV]		
					T = 145 K		0 K
					Calc	Exp	Calc
H_2	1/2	1/2	1/2	4155	80.1	74	**69.3** (*64.5*)
(H)D	1/3	2/3	2/3	3599	89.1	95	**78.9** (*74.5*)
H(D)	2/3	1/3	1/3	3599	48.4	46	**42.3** (*37.3*)
D_2	1/2	1/2	1/2	2939	61.3	70	**50.2** (*45.6*)

internal vibration being 74.5 meV. In fact the zero-point value at 0 K is always higher than that of internal vibration because of the effect of vibration and libration of the H_2, HD and D_2 molecules in a *solid lattice* formed on approaching 0 K. Moreover, the Debye temperature of e.g. solid H_2 and D_2 is quite high being 118 and 114 K respectively [21]. Accordingly, the zero point values at 0 K in Table 1 were calculated by assuming a pure Debye solid [22] where an average Debye temperature of 116 K was assumed for HD.

Table 1 shows also the experimental values of K_e(H) deduced by analyzing the results of ECS measurements [23], revealing large deviations of ~10% from the calculated values. To improve statistics we may consider the *sum* of the four measured K_e(H) values of Table 1 which differ by only 2% from that of the calculated sum. The deviations may be due to the assumptions and uncertainties involved in analyzing the data of [23]: (1) The temperature T of the reference gas (He) was estimated from the measured Doppler width of He to be 145 K indicating a huge drop in the gas temperature after leaving the needle near the electron beam. (2) The temperature T of H_2, HD and D_2 *was* assumed to be the same namely 145 K during the measurement. (3) The instrumental resolution was taken to be 0.2 eV and assumed to be the same for H_2, HD and D_2 at all incident e-energies between 1 and 6 keV.

3.2. The NH_3 molecule

The H-kinetic energy K_e(H) in ammonia is obtained by considering the geometry of the NH_3 molecule which has a pyramidal shape where the H-atoms form an equilateral triangle, with the N-atom at the top [24]. Here we also assume that the H-atom in NH_3 has three motions: translation, rotation and internal vibration which in the SE approach are assumed to be uncoupled. Hence K_e(H) for the vapor phase may be written as:

$$K_e(\mathrm{H}) = S_t\frac{3}{2}kT + S_r\frac{3}{2}kT + \sum_{j=1}^{6} S_j\frac{1}{2}\left(\frac{h\nu_j}{e^{h\nu_j/kT}-1}+\frac{h\nu_j}{2}\right) \quad (2)$$

The first two terms on the right of Eq. (2) represent the classical expression of translation and rotation of the entire molecule (each being $3kT/2$) with S_t and S_r the fractions shared by H-atom in those modes. The third term is the contribution of the six internal vibrational modes of the NH_3 molecule with frequencies ν_j. Note that S_j is the fraction of the kinetic energy shared by the H-atom in the jth vibrational mode; the factor 1/2 in the third term arises from the fact that in a harmonic oscillator, the kinetic energy is half its total energy. Table 2 lists the six measured internal vibrations frequencies [24,25] of $^{14}NH_3$ in its three phases. To calculate K_e(H) using Eq. (2), the main problem is to deduce the fractions S_j, obtained using computational methods of molecular spectroscopy described in [1,24]. Supplementary parameters resulting from such a calculation are the values of the spring constants which are also depicted in Table 2. In addition, the free rotations and translations of the vapor turn in the liquid and solid phases into librations and vibrations with frequency distributions $g_L(\nu)$ and $g_T(\nu)$ respectively. Thus K_e(H) in a condensed phase may be written as:

Table 2
Normal frequencies υ_j (j = 1,...,4) in units of cm^{-1} of $^{14}NH_3$ in the solid, liquid and *vapor* forms (taken from Refs. [27,28]) showing the frequency differences between the three phases. The corresponding spring constants k (in units of 10^5 dyn/cm) and the calculated fractions S_j of the kinetic energies of the H-atom are listed only for the *vapor* phase.

Normal modes	Solid	Liquid	Vapor	k_j	S_j
ν_1 (N—H sym stretch)	3217	3300	3336.2	5.8658	0.3251
$\nu_2 = \nu_3$ (H—N—H bend)	3371	3380	3443.3	0.3184	0.3104
ν_4 (H—H stretch)	1070	1060	950.2	0.2219	0.2824
$\nu_5 = \nu_6$ (H—H—H bend)	1626	1610	1627.8	0.6314	0.3096

$$K_e(H) = S_T\int_{\nu_{T0}}^{\nu_T} g_T(\nu)\alpha(\nu)d\nu + S_L\int_{\nu_{L0}}^{\nu_L} g_L(\nu)\alpha(\nu)d\nu + \sum_{j=1}^{3} S_j\frac{h\nu_j}{2}\left(\frac{1}{e^{h\nu_j/kT}-1}+\frac{1}{2}\right) \quad (3)$$

with $\alpha(\nu) = \frac{h\upsilon}{2}\left(\frac{1}{e^{h\nu/kT}-1}+\frac{1}{2}\right)$ the kinetic energy of the corresponding harmonic oscillator where ν_{T0}, ν_T, ν_{L0} and ν_L are the limits of integration; $g_T(\upsilon)$ and $g_L(\upsilon)$ are normalized so that:

$$\int_{\nu_{T0}}^{\nu_T} g_T(\nu)d\nu = \int_{\nu_{L0}}^{\nu_L} g_L(\nu)d\nu = 1 \quad (4)$$

Note that the $g_T(\nu)$ and $g_L(\nu)$ values for solid and liquid NH_3 are taken from inelastic neutron scattering (INS) data [26].

Fig. 2 displays the calculated values of K_e(H) for ammonia between 5 K and 300 K and applies to the gaseous, liquid and solid phases. Note that the calculated curve of the solid was smoothly joined continuously with that of the liquid and the vapor phases. The deviation from one curve to the other is less than 1%. The *classical* value of $K_e(H) = 3kT/2$ is also shown illustrating the huge contribution of the zero-point value of K_e(H) being 148 meV which constitutes the major part, ~98%, of the kinetic energy in the vapor phase at 200 K. The same nearly continuous behavior of the K_e(H) curve joining the three phases was also found in the case of water (see below). A good agreement may be seen between the calculated and the measured K_e(H) value at 80 K.

Note that the validity of the SE calculations was in fact established in a previous work [22] where the kinetic energy of the *N-atom* in NH_3 was studied using a different technique, namely the NRPS and an excellent agreement was obtained between the measured and SE calculations.

3.3. The water molecule

The calculation of K_e(H) for a triatomic H_2O molecule (in *vapor* form) proceeds in the same manner as in ammonia but has only 3 normal modes and was discussed in detail elsewhere [29]. In the liquid and solid case however, there is a major difference because the experimental vibrational modes are strongly influenced by the effect of the *hydrogen bonds* which weakens the OH stretch

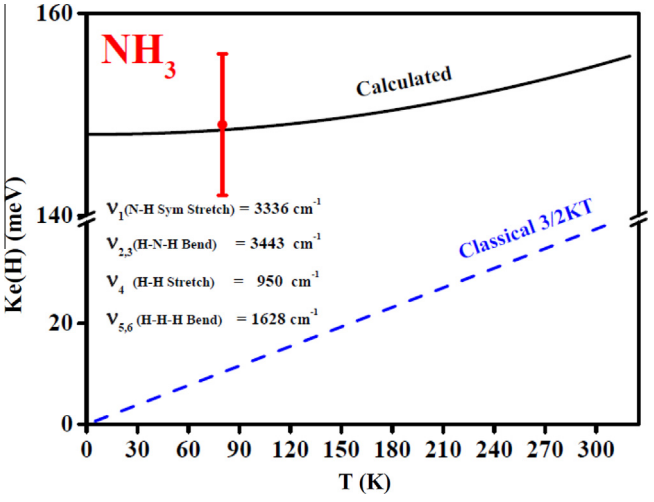

Fig. 2. Calculated K_e(H) values versus T for ammonia (NH_3) between 5 K and 320 K, covering the gaseous, liquid and solid phases. Note the slow increase of K_e(H) with T and the good agreement with the ECS measured preliminary value at 80 K (solid circle with error bar). The *classical* value $K_e(H) = 3kT/2$ is also shown revealing a huge difference from the present calculation which is due to the contribution of the zero-point motion. The K_e(H) value at 80 K was obtained by averaging the results for incident electrons of 1.5, 2.0 and 2.5 keV.

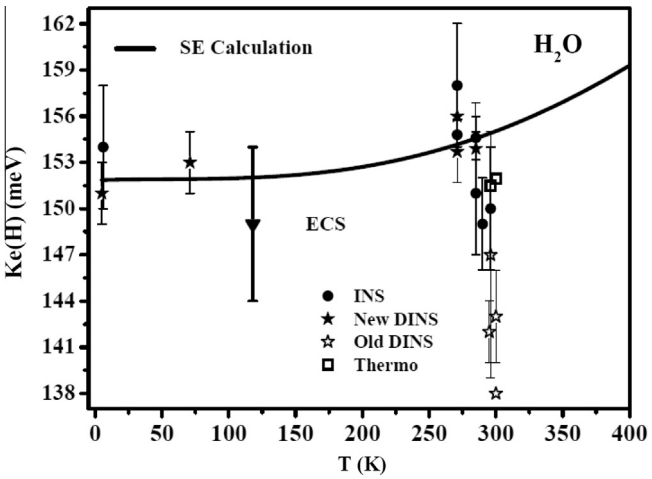

Fig. 3. Calculated K_e(H) values versus T for water (H_2O) between 5 K and 320 K, covering the liquid and solid phases. ECS measured value at 118 K is indicated (solid triangle) together with INS (solid circles) and DINS (solid and open stars) experimental values and theoretical predictions based on thermodynamic macroscopic data [29].

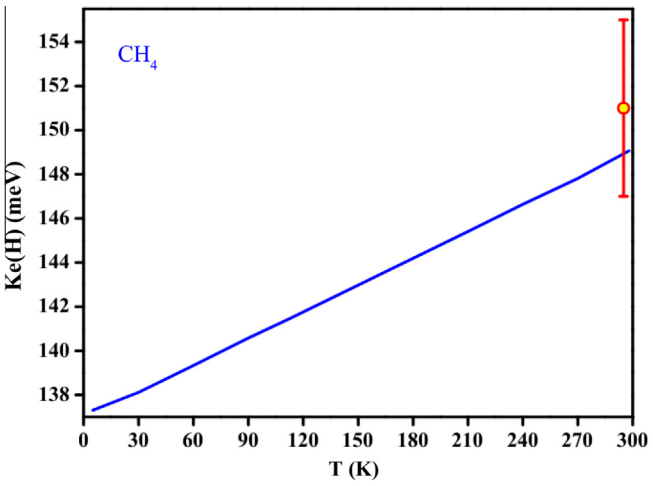

Fig. 4. Calculated K_e(H) values versus T for methane (CH_4) between 5 K and 300 K, covering the gaseous, liquid and solid phases. ECS measured value at 295 K is indicated. It was deduced by averaging over 6 measured values using different incident energies between 0.75 keV and 2.5 keV [4].

frequencies υ_j from 3686, 3738 cm^{-1} in the vapor, via 3280, 3490 cm^{-1} in the liquid to 3085 and 3220 cm^{-1} in ice Ih [29]. In addition, the free rotations and translations present in a *vapor* turn into librations and vibrations in the liquid and solid phases. The net effect of these opposing trends is to keep the calculated value of K_e(H) in water almost the same between 5 K and 300 K as may be seen in Fig. 3 which also shows the value, K_e(H) = 149 ± 5 meV measured for ice at 118 K using the e-scattering method [5]. The figure also displays several other measured values obtained using inelastic neutron scattering (INS) and deep inelastic neutron scattering (DINS). Note also in Fig. 3 the nearly *continuous* behavior of K_e(H) when passing between the various phases as was also found for ammonia and was discussed in detail in Ref. [29]. Table 3 summarizes the ECS measured and SE calculated K_e(H), K_e(D) and K_e(O) values in H_2O and D_2O.

3.4. Scattering intensities from the H- and D-atoms in water

One of the first high momentum transfer studies of electron scattering from solid H_2O and D_2O was published in Ref. [32] but no clear separation of H and O was possible. An important feature studied in the present work using the ECS method is the scattering intensities from H/D atoms relative to the O-atom in the molecule. This problem arose because of strong reported anomalies in the NCS method [11] when comparing the *neutron* scattering intensities from H:O in liquid H_2O with D:O in liquid D_2O at incident n-energies, E_n = 10–200 eV. An anomalous ~30% drop of the known n-H scattering intensity relative to the n-D scattering intensity was reported [11]. Because of the similarity between the NCS and ECS methods, it was interesting to test this anomaly using ECS [5]. Thus, the e-scattering intensity ratio of H to O in H_2O ice at 118 K was compared to the intensity ratio of D to O in D_2O. The results showed that the two ratios are equal [5], thus ruling out the existence of such anomaly with the ECS method. Another anomaly using NCS was reported in which the n-H scattering intensity was found to be smaller by ~30% compared to that of n-D scattering [13] in a sample of liquid HD at 20 K. However, the measured scattering intensities of n-H to n-D using the ECS method and a gaseous HD sample were found to be the same [23], thus no anomaly was revealed [14,33]. Another point worth noting in Ref. [14] concerns an additional drop in the scattering intensity ratio I_H/I_D of ~30% was reported in a gas mixture of $H_2 + D_2$. However, this was very probably caused by the different velocities of the two molecules H_2 and D_2 at the same temperature and not due to any real effect as explained in Ref. [34].

Table 3
Average measured and calculated K_e(H), K_e(D), and K_e(O) (in meV units) for ice Ih at 118 K in both H_2O and D_2O where errors are enclosed in parentheses. The incident electron energies were between 1.5 and 6.0 keV [5]. The calculation utilized optical frequencies together with the measured translational and librational spectra of solid [30] and liquid [31] water.

T (K)	H_2O				D_2O			
	K_e(H)		K_e(O)		K_e(D)		K_e(O)	
	Expt.	Calc.	Expt.	Calc.	Expt.	Calc.	Expt.	Calc.
118	149(5)	152.1(3)	34(2)	39.2(2)	97(3)	108.4(3)	43(2)	41.4(2)

3.5. The CH_4 molecule

The K_e(H) values of CH_4 were calculated in a similar manner to that of NH_3 by accounting for its 12 internal vibrational modes [16] and for the translational and librational frequencies of the solid phase [35]. The results vs T are plotted in Fig. 4 together with one measured value at 295 K obtained [4,36] using the ECS technique, K_e(H) = 151 ± 4 meV, revealing a good agreement with the calculations. This value is in fact an average over 6 measured values using different incident energies between 0.75 keV and 2.5 keV. Here again the ZPKE of the H-atom is also high but less pronounced than in H_2O and NH_3 because of the smaller contribution of its lattice frequencies revealing nearly free rotations at low T [37]; this is due to the highly spherical shape of CH_4.

4. Discussion

The electron scattering technique is now established as an important tool for studying a variety of topics including the measurement of the kinetic energies of H-atoms in several cases. It is of interest to note that the values of K_e(H) in the three molecules: NH_3, H_2O and CH_4 are practically the same at ~295 K. This is probably because the heavy partner has nearly the same mass in all three cases. The situation is different in the diatomic gases because the two partners are very light and the kinetic energy is divided

accordingly between the two atoms. Note that in Ref. [38] the zero-point *internal* vibrational energies of H_2, HD and D_2 were calculated by including anharmonic effects. It is interesting to compare the findings of [38] with the present results. Here, we assumed the harmonic approximation, calculated the *kinetic* part of ZPE per atom and included the effect of the *external* lattice vibration and libration. In [38], the *total* internal ZPE was calculated which is nearly twice the kinetic part; the inclusion of the anharmonic effects increased the ZPKE by ~4.4%. Here we included the contribution of the *external* lattice vibration and libration which amounted to ~10% of the ZPKE and was deduced by using the Debye temperature of the solid (see Table 1). This effect was not included in [38].

It is of interest to note that the ECS measured K_e(H) values are close to those obtained using the NCS. In H_2O, the K_e(H) value is practically constant between 5 K and 300 K as it is contributed by two compensating effects: one due to internal stretch vibrations which increases with T between 5 and 300 K and the second is due to the external vibrations which decreases with increasing T in the above T-range.

It was also shown that the calculation of K_e(H) using the SE approach can reproduce most experimental results measured by both the ECS and the NCS techniques. Moreover, it was possible to test some of the anomalies in neutron scattering from water reported using the NCS method.

Acknowledgements

We would like to thank Professor I. Bar for useful remarks. One of us (M.V) is grateful for a grant of the Australian Research Council.

References

[1] R. Moreh, O. Shahal, V. Volterra, Nucl. Phys. A 262 (1976) 221.
[2] J. Mayers, T.M. Burke, R.J. Newport, J. Phys. Condens. Matter 6 (1994) 641.
[3] D. Nemirovsky, R. Moreh, Y. Finkelstein, J. Mayers, J. Phys. Condens. Matter 13 (2001) 5053.
[4] M. Vos, J. Chem. Phys. 132 (2010) 074306.
[5] M. Vos, E. Weigold, R. Moreh, J. Chem. Phys. 138 (2013) 044307.
[6] M. Vos, R. Moreh, K. Tokesi, J. Chem. Phys 135 (2011) 024504.
[7] O. Shahal, R. Moreh, Phys. Rev. Lett. 40 (1978) 1714.
[8] R. Moreh, O. Shahal, Surf. Sci. 177 (1986) L963.
[9] R. Moreh, D. Levant, E. Kunoff, Phys. Rev. B 45 (1992) 742.
[10] Y. Finkelstein, O. Beck, R. Moreh, D. Jäger, U. Kneissl, J. Margraf, H. Maser, H.H. Pitz, Phys. Rev. B 58 (1998) 4166.
[11] C.A. Chatzidimitriou-Dreismann, T. Abdul-Redah, R.M.F. Streffer, J. Mayers, Phys. Rev. Lett. 79 (1997) 2839.
[12] C.A. Chatzidimitriou-Dreismann, M. Vos, C. Kleiner, T. Abdul-Redah, Phys. Rev. Lett. 91 (2003) 057403.
[13] C.A. Chatzidimitriou-Dreismann, T. Abdul-Redah, M. Krzystyniak, Phys. Rev. B 72 (2005) 054123.
[14] G. Cooper, A.P. Hitchcock, C.A. Chatzidimitriou-Dreismann, Phys. Rev. Lett. 100 (2008) 043204.
[15] R. Moreh, R.C. Block, Y. Danon, Phys. Rev. B 75 (2007) 057101.
[16] R. Moreh, D. Nemirovsky, J. Chem. Phys. 130 (2009) 174303.
[17] G. Gergely, M. Menyhard, Z. Benedek, A. Sulyok, L. Kover, J. Toth, D. Varga, Z. Berenyi, K. Tokesi, Vacuum 61 (2001) 107.
[18] A. Sulyok, G. Gergely, M. Menyhard, J. Toth, D. Varga, L. Kover, Z. Berenyi, B. Lesiak, A. Kosinski, Vacuum 63 (2001) 371.
[19] D. Varga, G. Gergely, A. Sulyok, Surf. Interface Anal. 31 (2001) 1019.
[20] G. Herzberg, Spectra of Diatomic molecules, D. Van Nostrand Co. Inc., Princeton, N.J., 1950.
[21] M. Nielsen, Phys. Rev. B 7 (1973) 1626.
[22] R. Moreh, O. Shahal, Phys. Rev. B 42 (1990) 913.
[23] M. Vos, M.R. Went, J. Phys. B: At. Mol. Opt. Phys. 42 (2009) 065204.
[24] G. Herzberg, Infrared and Raman Spectra, Van Nostrand Reinhold, New York, 1945.
[25] W.Y. Zenc, A. Anderson, Phys. Status Solidi (B) 162 (1990) 111.
[26] P.S. Goyal, B.A. Dasannacharya, C.L. Thaper, P.K. Iyengar, Phys. Status Solidi (B) 50 (1972) 701.
[27] O.S. Binbrek, A. Anderson, Chem. Phys. Lett. 15 (1972) 421.
[28] A. Bromberg, S. Kimel, A. Ron, Chem. Phys. Lett. 46 (1977) 262.
[29] Y. Finkelstein, R. Moreh, Chem. Phys. 431–432 (2014) 58.
[30] J. Li, J. Chem. Phys. 105 (1996) 6733.
[31] S.H. Chen, K. Toukan, C.K. Loong, D.L. Price, Phys. Rev. Lett. 53 (1984) 1360.
[32] F. Yubero, K. Tökèsi, Appl. Phys. Lett. 95 (2009) 084101.
[33] R. Moreh, D. Nemirovsky, J. Chem. Phys. 131 (2009) 054305.
[34] R. Moreh, Nucl. Inst. Meth. Phys. Res. B 279 (2012) 49.
[35] B.W. Baran, F.D. Medina, Chem. Phys. Lett. 176 (1991) 509.
[36] M. Vos, M.R. Went, G. Cooper, C.A. Chatzidimitriou-Dreismann, J. Phys. B: At. Mol. Opt. Phys. 41 (2008) 135204.
[37] R.M. Bansal, L.S. Kothari, S.P. Rewari, Phys. Lett. 33 (1970) 209.
[38] K.K. Irikura, J. Phys. Chem. Ref. Data 36 (2007) 389.